Available online at www.sciencedirect.com
ScienceDirect
Ceramics International 36 (2010) 1259–1263
CERAMICS INTERNATIONAL
www.elsevier.com/locate/ceramint

Carbon atmosphere effect on Ti_3SiC_2 based composites made from TiC/Si powders

Ida Kero *, Ragnar Tegman, Marta-Lena Antti

Luleå University of Technology, Department of Applied Physics, Mechanical and Materials Engineering, Division of Engineering Materials, SE-97187 Luleå, Sweden

Received 7 October 2009; received in revised form 23 October 2009; accepted 19 December 2009
Available online 28 January 2010

Abstract

The effect of carbon activity and CO pressure in the furnace atmosphere is investigated with respect to the phase reactions during heat treatment of TiC/Si powders. Special attention is given to the production and decomposition of Ti_3SiC_2. Samples were heated in graphite and alumina furnaces, connected to a dilatometer which enabled in situ analysis of the phase reactions. The phase compositions of the heat treated samples were determined by X-ray diffraction. The reducing atmosphere of the graphite furnace enhanced the reactivity of the starting powder and enabled phase reactions to take place at a lower temperature than in the alumina furnace. $TiSi_2$ and SiC phases formed at temperatures below the melting point of Si and were continuously consumed at higher temperatures. Ti_3SiC_2 formed at the melting point of Si regardless of furnace atmosphere. No decomposition of the Ti_3SiC_2 was observed in either furnace.

Keywords: A. Sintering; B. X-ray methods; C. Thermal expansion; D. Carbides

1. Introduction

The purpose of this study was to elucidate the impact of carbon activity and CO pressure in the furnace atmosphere on the phase reactions in a TiC/Si powder mixture, especially with respect to the Ti_3SiC_2 formation.

Ti_3SiC_2 based composites can be prepared by powder metallurgical methods from a variety of starting powders, many of which include Ti metal powder, such as Ti/Si/C [1–3] Ti/C/SiC [4–6] and Ti/Si/TiC [7–9]. Ti metal is very reactive and in the form of a powder it is even explosive in air, which makes it disadvantageous for up-scaled industrial production [10]. The binary carbides TiC and SiC have been shown to reinforce the Ti_3SiC_2, producing composites with enhanced oxidation resistance [11]. Both TiC– and SiC–Ti_3SiC_2 composites have been reported to possess high damage tolerance, flexural strength, fracture toughness and thermal shock resistance comparable with or even superior to monolithic Ti_3SiC_2 samples [12–15]. Ti_3SiC_2 based composites can be synthesised without the use of the hazardous Ti powder, and the phase composition can be adjusted by changing the Si content of the starting powder [1,16,17].

Authors working with other starting powders have suggested that the presence of carbon in the furnace atmosphere during heat treatment may be detrimental to the thermochemical stability of Ti_3SiC_2 [1,18], which has been assumed to decompose into TiC and gaseous Si [19]. Others have found that an addition of carbon powder may increase the purity of the Ti_3SiC_2 [2,20].

2. Materials and methods

The starting powders were TiC (Aldrich, <44 μm, 98%) and Si (Aldrich, <44 μm, 99%). The powders were mixed with a TiC/Si ratio of 3:2 corresponding to the stoichiometry of reaction (1):

$$3TiC + 2Si \leftrightarrow Ti_3SiC_2 + SiC \quad (1)$$

The powders were milled in a ball mill using propanol and zirconia spheres. The media diameter was 10 mm, the powder to media ratio was approximately 0.4 and the powder to propanol ratio was approximately 1.5. Powder particle size was

* Corresponding author. Tel.: +46 920 492 269; fax: +46 920 491 084.
E-mail address: ida.kero@ltu.se (I. Kero).

0272-8842/$36.00
doi:10.1016/j.ceramint.2010.01.016

estimated by SEM to be around 4 μm. The powder was then dried and compacted by uniaxial pressing to 10 MPa, and cold isostatic pressing (CIP) to 300 MPa, the initial density of the CIP:ed samples was calculated to be 70%. The samples had the shape of short cylinders of 10 mm diameter, approximately 3.5 mm in length and approximately 0.6 g in weight.

The green pellets were sintered in two different furnaces attached to a dilatometer. One furnace had a glass carbon protective tube and a graphite sample holder assembly; the other furnace had a protective tube and sample holder assembly of alumina. Sintering experiments were performed under a dynamic argon atmosphere with a gas flow rate approximately 85 ml/min, a heating rate of 10 K/min and a cooling rate of 20 K/min.

The dilatometric study was performed as follows: in a first step, a sample was heated up to 1500 °C in each furnace, in order to obtain a *global* dilatometric curve from which a number of points of interest could be determined. In order to assess whether a dilatational change was accompanied by any phase change green pellets were then heated up to temperatures in between the points of interest. The phase compositions of these heat treated samples were determined by X-ray diffractometry (XRD) using Cu radiation and a proportional detector. Heat treated samples were crushed into a powder before XRD analysis.

The phase fractions were determined using the direct comparison method [21], where the integrated intensity for a minimum of three diffraction lines of each phase were summed and the volume fractions of the individual phases were calculated using Eq. (2):

$$V_i = \frac{A_i}{A_\alpha + A_\beta + A_\gamma + \ldots} \text{ where } A_j = \sum_{j=1}^{n} \frac{I_j}{R_j} \tag{2}$$

where n is the number of *hkl* peaks for a given phase, V the volume fraction, I the integrated intensity, and R is the calculated theoretical intensity. Greek letters, α, β, $\gamma\ldots$ denotes the phases present. The validity of this procedure has been demonstrated for two-phase steels by Dickson [22].

3. Results and discussion

Fig. 1 shows the global dilatometric curves of samples heated to 1500 °C in the graphite and the alumina furnaces respectively. The linear cooling segments have been omitted for clarity. The two curves are similar in shape, the main difference is a temperature shift, as the curve of the sample heated in the alumina furnace exhibits the same features as that in the graphite furnace but every feature occurs at a higher temperature.

The difference between the two furnaces may be explained by the strongly reducing atmosphere in the graphite furnace. The powder particles have probably formed a thin oxide layer on the Si particle surfaces when exposed to air; as this oxide is quite chemically stable it will slow down any chemical reaction between the Si of the particle and its surroundings. In the graphite furnace, water molecules adhering to surfaces in the

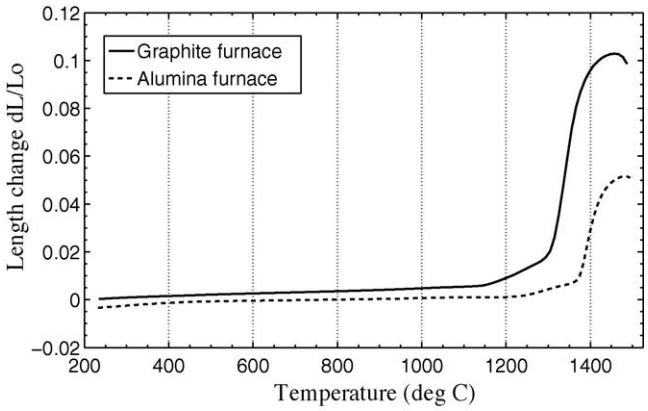

Fig. 1. Dilatometer curves of the two furnaces.

powder and in the furnace will react with graphite to form carbon monoxide gas at elevated temperatures:

$$H_2O + C(s) \leftrightarrow CO(g) + H_2(g) \tag{3}$$

Carbon monoxide gas is very reducing and the oxide layer will be attacked by it:

$$CO(g) + SiO_2(s) \leftrightarrow SiO(g) + CO_2(g) \tag{4}$$

In the dynamic furnace atmosphere, the argon flow will flush out the formed CO_2- and SiO-gas, leaving clean Si particle surfaces. As Si is more reactive than SiO_2, this process will enable earlier reactions. The reducing capacity of the furnace remains unchanged however, as the CO_2 thus formed will react with the graphite of the furnace to release more CO gas:

$$CO_2(g) + C(s) \leftrightarrow 2CO(g) \tag{5}$$

As the alumina furnace atmosphere is not of a reducing character, a higher temperature is required for phase reactions to take place.

From Fig. 1 the following points of interest may be distinguished: the thermal expansion is linear up to 1142 and 1234 °C in the graphite and the alumina furnaces respectively. There are peak onsets at 1276 and 1363 °C, and the peak reaches a maximum at 1457 and 1483 °C respectively. The phases present at each temperature examined in the graphite and alumina furnaces are summarized in Tables 1 and 2 respectively. After the peak, the sample shrinks abruptly and silicon may be given off. In order to avoid excessive silicon evaporation and instrument contamination, the heating segment was limited to 1500 °C.

Table 1
Temperatures and phase compositions of samples heat treated in the graphite furnace.

Graphite furnace dilatometer	
Temperature (°C)	Phases present
1115	TiC, Si
1260	TiC, Si, SiC, $TiSi_2$
1390	TiC, Si, SiC, $TiSi_2$
1415	TiC, SiC, Ti_3SiC_2, $TiSi_2$
1500	TiC, SiC, Ti_3SiC_2

Table 2
Temperatures and phase compositions of samples heat treated in the alumina furnace.

Alumina furnace dilatometer	
Temperature (°C)	Phases present
1170	TiC, Si, $TiSi_2$
1290	TiC, Si, SiC, $TiSi_2$
1410	TiC, SiC, Ti_3SiC_2, $TiSi_2$
1450	TiC, SiC, Ti_3SiC_2, $TiSi_2$
1500	TiC, SiC, Ti_3SiC_2, $TiSi_2$

Fig. 2 shows X-ray diffractograms of samples heated in the graphite furnace. TiC was present at all temperatures. In the graphite furnace $TiSi_2$ peaks are observed from 1260 °C, likely corresponding to the loss of dilatational linearity at 1142 °C. Ti_3SiC_2 peaks are observed from 1415 °C and a Ti_3SiC_2 producing reaction is therefore likely to correspond to the dilatometric peak.

Fig. 3 shows the variations in volume fraction of the different phases present in the graphite furnace as a function of temperature. The Ti_3SiC_2 appears at 1415 °C and the content increases with temperature. $TiSi_2$ appears at 1260 °C, its volume fraction peaks at 1415 °C after which it disappears.

Fig. 4 shows the X-ray diffractograms of samples sintered in the alumina furnace. $TiSi_2$ and TiC are present at all temperatures. From the dilatometer curve in Fig. 1, $TiSi_2$ would be expected to form at temperatures above 1230 °C in the alumina furnace, but it is detected in small amounts at 1170 °C which is likely an effect of minor inhomogeneities of the initial TiC/Si powder.

Fig. 5 shows the variations in volume fraction of the different phases present in the alumina furnace as a function of temperature. Ti_3SiC_2 is present at 1410 °C and the amount increases with temperature. The $TiSi_2$ volume fraction is highest at 1290 °C but remains fairly constant until 1450 °C after which it decreases.

The $TiSi_2$ and SiC are the first phases to form in both furnaces and they both appear to decrease with increasing temperature. The SiC phase amount reaches a maximum at 1260 and 1290 °C in the graphite and alumina furnaces respectively. $TiSi_2$ is completely consumed at 1500 °C in the graphite furnace but remains in small amounts in samples sintered in the alumina furnace at the same temperature. $TiSi_2$ and SiC are most likely formed by reaction (6):

$$TiC + 3Si \leftrightarrow TiSi_2 + SiC \quad (6)$$

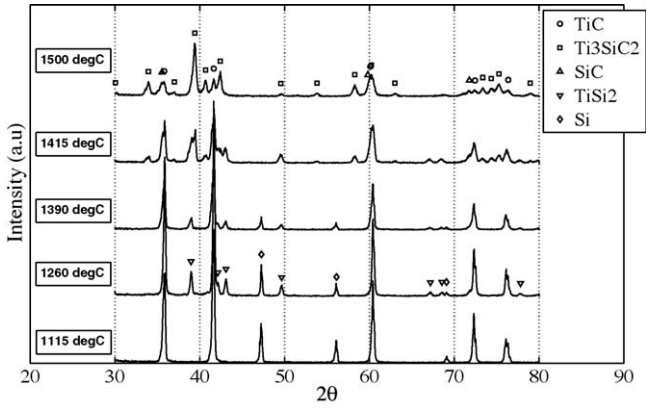

Fig. 2. X-ray diffractograms of samples sintered in the dilatometer with graphite furnace.

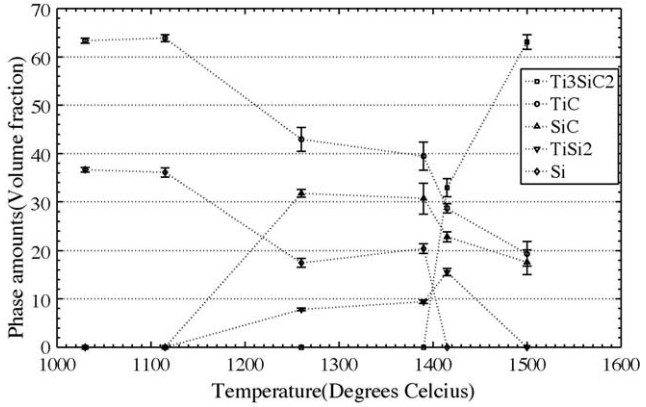

Fig. 3. Volume fraction of the different phases at the different temperatures in the graphite furnace.

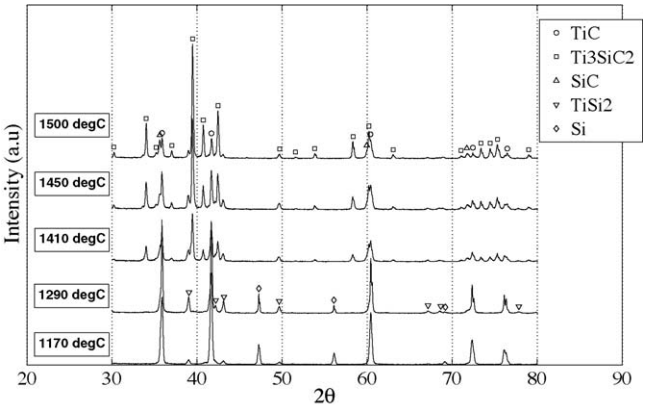

Fig. 4. X-ray diffractograms of samples sintered in the dilatometer with alumina furnace.

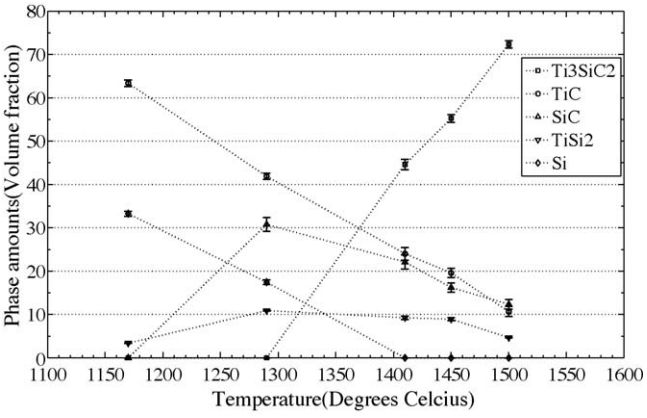

Fig. 5. Volume fraction of the different phases at the different temperatures in the alumina furnace.

Ti_3SiC_2 was formed in both furnaces, the alumina furnace produced a slightly higher amount of Ti_3SiC_2 than the graphite furnace (72.3 vol% ± 0.8 which corresponds to 90.5 mol% in the alumina furnace and 63.1 vol% ± 1.5 corresponding to 87.5 mol% in the graphite furnace). The Ti_3SiC_2 phase seems to be produced at approximately the same temperature regardless of furnace atmosphere and the volume fraction increases with temperature. The temperature of production is 1410 and 1415 °C in the alumina and the graphite furnaces respectively, this is approximately the melting temperature of Si (Si melts at 1414 °C [23]). A liquid phase enhances wetting and increases diffusion rate, thereby enabling reaction (1).

The Ti_3SiC_2 content increased unstintingly with increasing temperature in both furnaces and it showed no sign of decomposition at the temperatures examined. Si evaporation had previously been observed in samples similar to those examined in this study. This occurred at temperatures higher than 1500 °C which appears to corroborate the results of Racault et al. [19] who found that Si was given off at high temperatures and most notably so in the presence of graphite. They observed Si evaporation from 1300 and 1450 °C in graphite and alumina furnaces respectively and suggested that the process would be a result of the decomposition of Ti_3SiC_2 by carburisation. This is not, however, consistent with our results where no decomposition was found to occur at these temperatures in either furnace. Although more Ti_3SiC_2 was produced in the alumina furnace, molar balance calculations suggest only minor losses of Si from the samples examined in this study.

From Figs. 3 and 5 it is clear that the phase amounts of TiC, $TiSi_2$ and SiC decreases as the Ti_3SiC_2 amount increases. It is suggested that $TiSi_2$ may be consumed by reaction (7) which also accounts for the continued Ti_3SiC_2 production after all the Si is consumed.

$$7TiC + 2TiSi_2 \leftrightarrow 3Ti_3SiC_2 + SiC \quad (7)$$

At very high temperatures, the partial pressure of Si in the furnace atmosphere may become large enough to allow Si gas to form. The Si gas would then be flushed out with the argon. From the results of this study, the Si vapour is suggested to form as a result of reaction (8):

$$3TiSi_2 + 2SiC \leftrightarrow Ti_3SiC_2 + 7Si(g) \quad (8)$$

We thus propose a cascade of phase reactions:

$$TiC + 3Si \leftrightarrow TiSi_2 + SiC \quad (6)$$

$$3TiC + 2Si \leftrightarrow Ti_3SiC_2 + SiC \quad (1)$$

$$7TiC + 2TiSi_2 \leftrightarrow 3Ti_3SiC_2 + SiC \quad (7)$$

$$3TiSi_2 + 2SiC \leftrightarrow Ti_3SiC_2 + 7Si(g) \quad (8)$$

where reaction (6) would be the first to take place at temperatures below the melting point of silicon. Reactions (1) and (7) would be enabled by the liquid phase diffusion in the molten Si, and thereby occur more or less simultaneously. As reactions (1) and (6) are limited by the access to Si, they must come to an end earlier than reaction (7). Finally, reaction (8) may occur at very high temperatures, when Si vapour pressure is large enough.

4. Conclusions

The impact of carbon activity and CO pressure in the furnace atmosphere was studied with respect to the phase reactions in a TiC/Si powder mixture, special attention was given to the formation and decomposition of Ti_3SiC_2.

The reducing nature of the atmosphere in a graphite furnace was found to increase the starting powder reactivity and enabled phase reactions to take place at a lower temperature than in an alumina furnace.

$TiSi_2$ and SiC phases were found to form at temperatures below the melting point of Si. These phases were continuously consumed at higher temperatures. $TiSi_2$ was completely consumed in the graphite furnace at 1500 °C while it remained present at all temperatures investigated in the alumina furnace.

Ti_3SiC_2 formed at the melting point of Si regardless of furnace atmosphere. The enhanced wetting and diffusion rate in the liquid is assumed to be necessary for the Ti_3SiC_2 forming reactions to take place, at a heating rate of 10 K/min. More Ti_3SiC_2 was produced in the alumina furnace than in the graphite furnace.

No decomposition of the Ti_3SiC_2 was observed in either furnace and only minor losses of silicon through evaporation could be established at temperatures below 1500 °C.

Acknowledgements

I. Kero gratefully acknowledges financial support from the Swedish National Graduate School of Space Technology.

References

[1] R. Radhakrishnan, J.J. Williams, M. Akinc, Synthesis and high-temperature stability of Ti_3SiC_2, Journal of Alloys and Compounds 285 (1999) 85–88.
[2] S.-B. Li, J.-X. Xie, L.-T. Zhang, L.-F. Cheng, Synthesis and some properties of Ti_3SiC_2 by hot pressing of titanium, silicon and carbon powders. Part 1—Effect of starting composition on formation of Ti_3SiC_2 and observation of Ti_3SiC_2 crystal morphology, Materials Science and Technology 10 (19) (2003) 1442.
[3] Y. Zhou, Z. Sun, Temperature fluctuation/hot pressing synthesis of Ti_3SiC_2, Journal of Materials Science 35 (2000) 4343–4346.
[4] T. El-Raghy, M.W. Barsoum, Processing and mechanical properties of Ti_3SiC_2: I. Reaction path and microstructure evolution, Journal of the American Ceramic Society 10 (82) (1999) 2849–2854.
[5] E. Wu, E.H. Kisi, D.P. Riley, R.I. Smith, Intermediate phases in Ti_3SiC_2 synthesis from Ti/SiC/C mixtures studied by time-resolved neutron diffraction, Journal of the American Ceramic Society 12 (85) (2002) 3084–3086.
[6] P.V. Istomin, A.V. Nadutkin, I. Ryabkov, B.A. Goldin, Preparation of Ti_3SiC_2, Inorganic Materials 3 (42) (2006) 250–255.
[7] S. Yang, Z.M. Sun, H. Hashimoto, Synthesis of Ti_3SiC_2 powder from 1Ti/(1 − x)Si/2TiC powder mixtures, Journal of Alloys and Compounds 368 (2004) 318–325.
[8] J.T. Li, Y. Miyamoto, Fabrication of monolithic Ti_3SiC_2 ceramic through reactive sintering of Ti/Si/2TiC, Journal of Materials Synthesis and Processing 2 (7) (1999) 91–96.

[9] N.F. Gao, Y. Miyamoto, D. Zhang, On physical and thermochemical properties of high-purity Ti_3SiC_2, Materials Letters 55 (2002) 61–66.
[10] E. Poulsen, Safety-related problems in the titanium industry in the last 50 years, JOM: The Member Journal of TMS 5 (50) (2000) 13–17.
[11] S. Li, J. Xie, L. Zhang, L.-F. Cheng, Mechanical properties and oxidation resistance of Ti_3SiC_2/SiC composite synthesised by in situ displacement reaction of Si and TiC, Materials Letters 57 (2003) 3048–3056.
[12] L.H. Ho-Duc, T. El-Raghy, M.W. Barsoum, Synthesis and characterization of 0.3 V_f TiC–Ti_3SiC_2 and 0.3 V_f SiC–Ti_3SiC_2 composites, Journal of Alloys and Compounds 350 (2003) 303–312.
[13] J. Zhang, L. Wang, W. Jiang, L. Chen, Effect of TiC on the microstructure and properties of Ti_3SiC_2–TiC composites in situ fabricated by spark plasma sintering, Materials Science and Engineering A 487 (2008) 137–143.
[14] J. Zhang, T. Wu, L. Wang, W. Jiang, L. Chen, Microstructure and properties of Ti_3SiC_2/SiC nanocomposites fabricated by spark plasma sintering, Composites Science and Technology 68 (2008) 499–505.
[15] S.S. Hwang, S.W. Park, T.W. Kim, Mechanical properties of synthesized Ti_3SiC_2 by hot pressing from TiC_x/Si powder, Mixture Key Engineering Materials 287 (2005) 194–199.
[16] S.-B. Li, J.-X. Xie, L.-T. Zhang, L.-F. Cheng, In situ synthesis of Ti_3SiC_2/SiC composite by displacement reaction of Si and TiC, Materials Science and Engineering A 381 (2004) 51–56.
[17] I. Kero, R. Tegman, M.-L. Antti, Effect of the amounts of silicon on the in situ synthesis of Ti_3SiC_2 based composites made from TiC/Si powder mixtures, Ceramics International 36 (1) (2010) 375–379.
[18] E. Wu, E.H. Kisi, S.J. Kennedy, A.J. Studer, In situ neutron powder diffraction study of Ti_3SiC_2 synthesis, Journal of the American Ceramic Society 10 (84) (2001) 2281–2288.
[19] C. Racault, F. Langlais, R. Naslain, Solid-state synthesis and characterization of the ternary phase Ti_3SiC_2, Journal of Materials Science 29 (1994) 3384–3392.
[20] S. Arunajatesan, A.H. Carim, Synthesis of titanium silicon carbide, Journal of the American Ceramic Society 3 (78) (1995) 667–672.
[21] B.D. Cullity, Elements of X-ray diffraction, in: M. Cohen (Ed.), Addison-Wesley Series in Metallurgy and Materials, 3rd ed., Addison-Wesley Publishing Company, Inc., 1956.
[22] M.J. Dickson, The significance of texture parameters in phase analysis by X-ray diffraction, Journal of Applied Crystallography 176–180 (2) (1969).
[23] D.R. Lide, CRC Handbook of Chemistry and Physics, Florida, Boca Raton, 1999.